Volume 5, Number 2 ACTA PHYSICA SINICA February, 1996
1004-423X/96/05020126-17 (Overseas Edition) © 1996 Chin. Phys. Soc.

# MAGNETIC POLARIZATION OF Pd SPACERS AND OSCILLATORY EXCHANGE COUPLING BETWEEN Fe AND Pd LAYERS IN Fe/Pd MULTILAYERS*

MEI LIANG-MO(梅良模), LI MIN(李 民), XIE SHI-JIE(解士杰), and LIU YI-HUA(刘宜华)
*Department of Physics, Shandong University, Jinan 250100, China*

XU RONG-LI(徐荣历)
*Department of Mathematic Physics, Shandong Industrial University, Jinan 250014, China*

(Received 24 January 1995)

An oscillatory behavior in specific saturation magnetization of Fe/Pd multilayers is observed. The conversion electron Mössbauer spectroscopy and other experiments indicate that this behavior is caused by the magnetic polarization of Pd spacers, which alternates between positive and negative polarization with respect to the magnetic moments of Fe layers. The interlayer coupling between two Fe layers always keeps ferromagnetic. Then, the interlayer couplings in ferromagnetic metal/nearly ferromagnetic metal multilayers were calculated by using the model of Barnas. The results of calculation prove that the above phenomenon might appear under some condition. The influence of magnetic polarization potential of spacers and interface chemical potential on the interlayer couplings is also discussed.

**PACC:** 7570; 7680; 7550B; 7530E

## I. INTRODUCTION

The magnetic behavior of a magnetic multilayer structure may differ in many respects from those of a single layer films and a bulk solid. This is due to the fact that the reduced symmetry near interface, highly localized interface states, interlayer coupling and lower dimension offer the possibility of inducing new interesting magnetic structures and phenomena. So the study of magnetic multilayer has emerged as one of the most active areas of condensed matter. In recent years, both exchange coupling and saturation magnetoresistance oscillations as a function of non-magnetic spacer layer thickness have been observed in Fe/Cr, Co/Cu and Co/Ru multilayer or sandwich structures.[1-5] Several mechanisms of the coupling have been proposed to account for the experimental data, including the RKKY-type coupling via conducting electrons of a spacer[6-8], coupling through d electrons of the interlayer[9-12], coupling due to hybridization of the conducting electron states in the spacer with the interface d electron states of the magnetic layers[13,14] and a spin-polarized free-electron approximation model for the conducting electrons in both ferromagnetic layers

*Project supported by the National Natural Science Foundation of China, the Doctoral Foundation of National Education Commission of China and by State Key Laboratory of Magnetism, Chinese Academy of Sciences.

and non-magnetic spacer.[15] In all these reported cases, it was assumed that the spacer layer has no contribution of magnetic moment to the layered structures. The spin polarization effect of the spacers and its influence on the interlayer coupling are not well understood and needed to be studied.

Paramagnetic palladium is sometime called "nearly ferromagnetic metal" because of the quite large Stoner enhancement factor ($S = 10$). There are many strange phenomena in the alloys consisting of palladium and ferromagnetic elements. For example, Fe atom in diluted FePd alloys shows a giant magnetic moment[16], FePdPt solid solutions show a variety of magnetic phases (ferromagnetic, ferrimagnetic and antiferromagnetic) with the varying of palladium composition.[17] So Fe/Pd multilayer structure is a good system for studying interlayer coupling. Stoffler and Gautier[11] have studied a multilayer structure with nearly ferromagnetic metallic spacer ($Co_4Pd_n$), using the mechanism of coupling through d electrons of the interlayer. The conclusion[14] is that for a small Pd thickness ($n < 4$) all Pd atoms are ferromagnetically coupled to Co and a ferromagnetic coupling occurs between magnetic layers; and for a larger Pd thickness ($n > 4$) an oscillatory behaviour of interlayer coupling appears. However, Parkin has found no evidence for the existence of such an oscillatory exchange coupling in the multilayer structures with Pd and Pt.[18] Celiski et al.[19] have studied the interlayer coupling in Fe/Pd/Fe trilayers and observed the antiferromagnetic coupling between Fe layers for a quite large Pd spacer thickness. This indicates that the results are not in accordance with each other and further investigation is needed. In the present paper, the X-ray diffraction (XRD), vibrating sample magnetometer (VSM), conversion electron Mössbauer spectroscopy (CEMS) studies on Fe/Pd multilayers and theoretical analysis based on the model of Barnas are presented and comparison between experiment and theory is also given.

## II. EXPERIMENTAL

The multilayered structures were prepared in a vacuum vapor deposition system with a background pressure of about $4 \times 10^{-6}$ Torr. The deposition rates of Fe and Pd were 0.05 nm/s and 0.075 nm/s, respectively, monitored with a quartz resonator. Four series, each having 40 bilayers, of structures were grown on 0.1 mm thick glass slides via computerized control of shutters.

The layered structure was checked by small angle XRD and the crystallinity of samples was investigated by high angle XRD. The magnetic properties of the multilayer samples were measured by using VSM in the temperature range of 77–1000 K. A magnetic field up to 1 kOe was applied in the plane of the sample. From the magnetization curve, one can see that this field is large enough to saturate the samples. The room temperature $^{57}Fe$ conversion

electron Mössbauer spectra were recorded by using a gas-flow ($CH_3COCH_3$) proportional counter. The spectrometer was calibrated with a standard $\alpha$-Fe foil. The spectra were fitted by using the standard MUSFUN program on a PDP11/34 computer system.

## III. RESULTS AND DISCUSSIONS

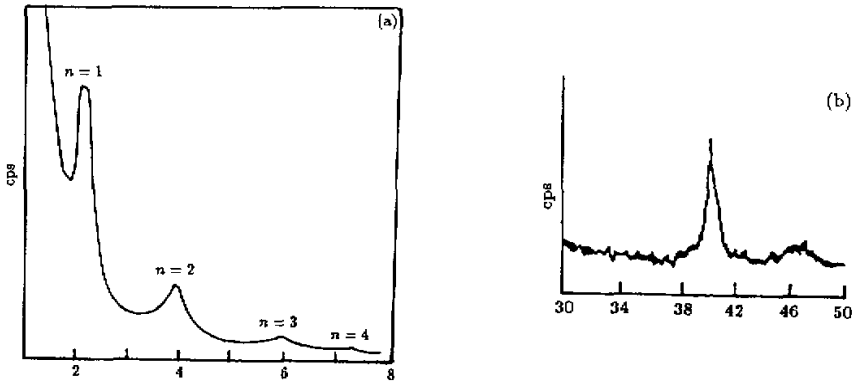


(a) Small angle XRD (b) High angle XRD

**Fig. 1.** Typical XRD patterns.

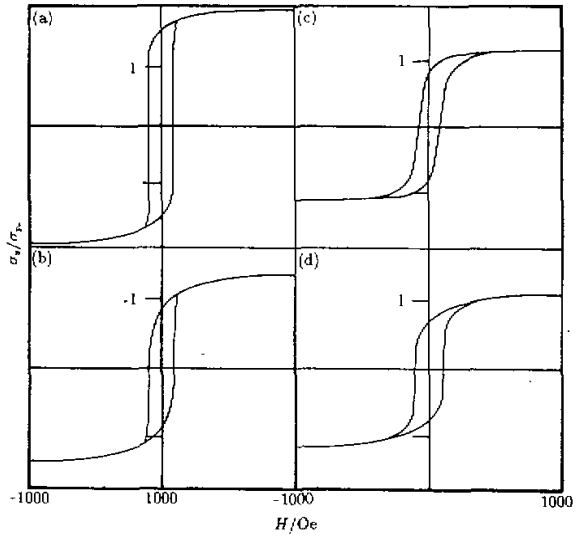


**Fig. 2.** The typical room-temperature magnetic hysteresis loops of [Fe(0.6–6.0 nm)/Pd(3.0 nm)]$_{40}$ multilayers. (a) $d_{Fe} = 0.57$ nm; (b) $d_{Fe} = 1.6$ nm; (c) $d_{Fe} = 3.7$ nm; (d) $d_{Fe} = 5.6$ nm.

Figure 1 shows the typical XRD patterns. In small angle XRD patterns [Fig. 1(a)], four peaks could be seen. It indicates that the films have good layered periodicity. However, the diffraction peaks are not sharp, especially the first one, and this indicates an unsmoothed interface. The modulated wavelengths determined by small angle XRD are in good agreement ($< 5\%$) with the nominal values. High angle XRD data show that the films are fcc polycrystalline with (111) texture, and that the (111) XRD peaks of the films are located around Pd (111) position. This indicates that the lattice of Fe layers shows large mismatch.

Figure 2 shows the typical room-temperature magnetic hysteresis loops of [Fe(0.6–6.0 nm) /Pd(3.0 nm)]$_{40}$ multilayer samples. It can be seen that the applied field, 1 kOe, is high enough to saturate the samples. The specific saturation magnetization, $\sigma_s$, obtained from the magnetic hysteresis loops measurements, versus Fe layer thickness, $d_{Fe}$ for [Fe(0.6–6.0 nm)/Pd(3.0 nm)]$_{40}$ multilayer samples at room temperature or 0 K are shown in Fig. 3(a). The specific magnetization at 0 K, $\sigma_s(0)$, was obtained by means of fitting the experimental data with formula $\sigma_s(T) = \sigma_s(0)(1 - BT^{3/2})$. The $\sigma_s$ increases with the decrease of Fe layer thickness, $d_{Fe}$, monotonously, and shows a linear dependence on $1/d_{Fe}$ over 0.6–6.0 nm range [Fig. 3(b)]. So the relation between $\sigma_s(T)$ and $d_{Fe}$ can be written as

$$\sigma_s(T) = \sigma_s^{Fe}(T) + \alpha \frac{1}{d_{Fe}} , \tag{1}$$

where $\sigma_s^{Fe}(T)$ is the specific saturation magnetization of 200 nm Fe single layer, or the intersecting point of the backward extrapolated $\sigma_s$-$1/d_{Fe}$ line with $\sigma_s$ axis, and $\alpha$ the line slope ratio.

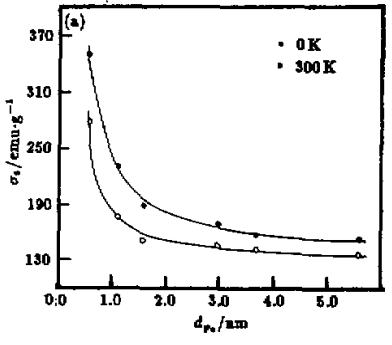


(a) The dependences of the specific saturation magnetization of [Fe(0.6–6.0 nm)/Pd (3.0 nm)]$_{40}$ on magnetic layer thickness $d_{Fe}$.

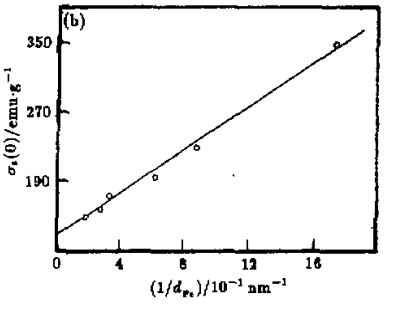


(b) The specific saturation magnetization of [Fe(0.6–6.0 nm)/Pd(3.0 nm)]$_{40}$ as a function of $1/d_{Fe}$ at 0 K.

**Fig. 3.**

For studying the magnetization enhancement in [Fe(0.6–6.0 nm)/Pd(3.0 nm)]$_{40}$ multilayered structures, conversion electron Mössbauer spectra were recorded, as shown in Fig. 4. The Mössbauer spectrum of a single Fe layer film is also shown in Fig. 4 for comparison.

The lines of CEMS sixlet of $[Fe/Pd(3.0\,nm)]_{40}$ are asymmetric and their linewidths are wider than those of Fe single layer. The computer fitting of the spectra gave out two sets of the average Mössbauer parameters which are listed in Table 1. The first set of parameters is about the same as that of Fe single layer. It means that the states of intralayer Fe atoms in multilayer structures have no change, compared with that in a single layer.

**Table 1.** Computer fitting Mössbauer parameters.

| | First set | | | Second set | | |
|---|---|---|---|---|---|---|
| | $H_{hf}$/kOe | IS/mm·s$^{-1}$ | WS/mm·s$^{-1}$ | $H_{hf}$/kOe | IS/mm·s$^{-1}$ | WS/mm·s$^{-1}$ |
| Fe(200 nm) | 330.0 | 0.01 | 0.20 | | | |
| Fe(5.6 nm)/Pd(3.0 nm) | 331.7 | 0.02 | 0.20 | 324.8 | 0.154 | 0.54 |
| Fe(3.7 nm)/Pd(3.0 nm) | 331.8 | 0.01 | 0.21 | 324.9 | 0.152 | 0.60 |
| Fe(3.0 nm)/Pd(3.0 nm) | 332.3 | 0.01 | 0.20 | 324.1 | 0.160 | 0.57 |

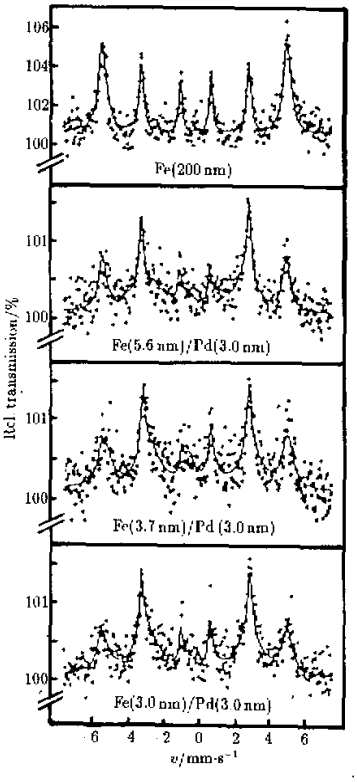


**Fig. 4.** The conversion electron Mössbauer spectra of $[Fe(0.6–6.0\,nm)/Pd(3.0\,nm)]_{40}$ and a single layer Fe film (room temperature).

The hyperfine field of the second set is slightly lower than that of the single layer, and the isomer shift moves toward positive slightly. Such a kind of slight changes in the second set of parameters could be attributed to that Fe atoms in the interface region meet broken symmetry. According to the ratio of the sections of the two sets of spectra, the percentage of Fe atoms at the interface can be obtained as 9%, 13.5%, and 17.7% for $d_{Fe} = 5.6, 3.7$, and 3.0 nm, respectively, while the interface Fe layer thicknesses are 0.46 nm, 0.44 nm and 0.45 nm. That is to say, in Fe/Pd multilayers the interface Fe layer thickness for one side is about 0.22–0.23 nm. From the data in Table 1, the hyperfine field is 2% smaller than that of the inner parts of Fe layers. The magnetization of Fe layers have no additional contribution to the observed enhanced magnetization in $[Fe(0.6–6.0\,nm)/Pd(3.0\,nm)]_{40}$ structures. Therefore it may be reasonable to assume that Pd atoms in the spacer are magnetically polarized by RKKY-like interaction with Fe atoms at the interface region and contribute their moments to the samples. Under such an assumption, the enhanced magnetization arising from the parallel polarization of Pd spacers could be equivalently and approximately described as an increment of Fe layer thickness in multilayer structures. Then, Eq. (1) can be rewritten as

$$\sigma_s(T) = \sigma_s^{Fe}(T)(1 + \frac{\Delta d(T)}{d_{Fe}}) , \tag{2}$$

where $\Delta d$ is the equivalent increment of Fe layer thickness. Based on the experimental data, $\Delta d$ does not depend on the Fe layer thickness $d_{Fe}$, but depends on temperature. At a given temperature, $\Delta d$ is a constant. For example, at 0 K $\Delta d = 1.0$ nm was evaluated by fitting the experimental data with Eq. (2). In other words, 0.5 nm increment of Fe layer thickness at each interface is caused by the positive polarization of Pd layer equivalently. The temperature dependence of $\Delta d$ is shown in Fig. 5. With computer fitting, one can get

$$\Delta d(T) = aT + b , \tag{3}$$

where $a = -1.75 \times 10^{-3}$ nm·K$^{-1}$, $b = 0.97$ nm.

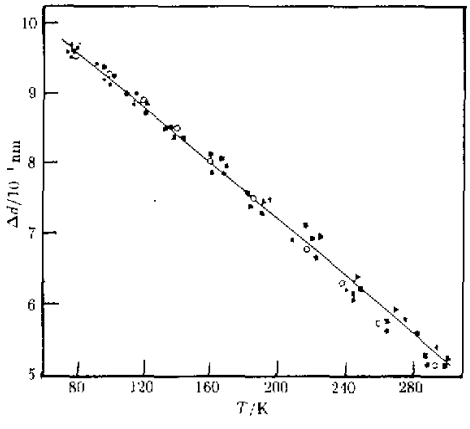


**Fig. 5.** Temperature dependence of $\Delta d$ in $[Fe(0.6–6.0\,nm)/Pd(3.0\,nm)]_{40}$ structures (77–300 K). $d_{Fe} = 0.57$ nm (■); 1.10 nm (*); 1.60 nm (+); 3.00 nm (○); 3.70 nm ( ▲ ); 5.60 nm (●); $d_{Pd} = 3.00$ nm.

Moriya has reported that the magnetic polarization of Pd atoms oscillates with the distance of Pd-Fe atoms with respect to the magnetic moment of Fe atoms. The high angle XRD has indicated that the Fe layers have larger mismatch. Then it can be speculated that the degree of mismatch of Fe layers varies with the thickness of Pd layer, and hence the Pd-Fe atomic distance will be varied. This may influence the magnetic polarization of Pd atoms. For studying the relationship between magnetic polarization of Pd layers and Pd layer thickness, the magnetic properties of $[Fe(0.6–6.0\,nm)/Pd(2.0\,nm)]_{40}$ multilayers were measured. Figure 6 shows the dependence of specific saturation magnetization $\sigma_s$ of $[Fe(0.6–6.0\,nm)/Pd(2.0\,nm)]_{40}$ structures on Fe layer thickness at room temperature. Its behaviour is completely different from that of $[Fe(0.6–6.0\,nm)/Pd(3.0\,nm)]_{40}$. In this case,

the $\sigma_s$ decreases with the decrease of Fe layer thickness and is smaller than the value of Fe single layer. This means that in $[Fe(0.6–6.0\,nm)/Pd(2.0\,nm)]_{40}$ structures the $d$ layer is negatively polarized. By fitting the data in Fig. 6 with formula (2), one can get that $\Delta d \approx -0.6\,nm$, i.e., 0.3 nm decrement of Fe layer thickness at each interface can be caused by the negative polarization of Pd layer. Hence, as the Pd layer thickness in $[Fe/Pd]_{40}$ structures changes from 3.0 to 2.0 nm, the magnetic polarization of Pd spacer will change from positive to negative, i.e., from ferromagnetic coupling to antiferromagnetic coupling with Fe layers.

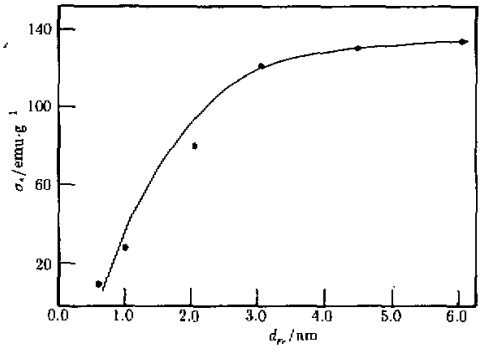


**Fig. 6.** Dependence of specific saturation magnetization on magnetic layer thickness in $[Fe(0.6–6.0\,nm)/Pd(2.0\,nm)]_{40}$ (room temperature).

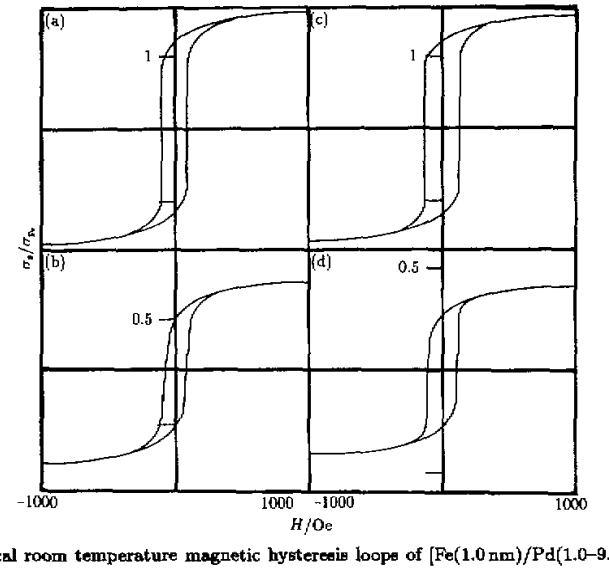


**Fig. 7.** Typical room temperature magnetic hysteresis loops of $[Fe(1.0\,nm)/Pd(1.0–9.0\,nm)]_{40}$ and $[Fe(2.0\,nm)/Pd(1.0–9.0\,nm)]_{40}$ multilayers. $d_{Fe} = 1.0\,nm$, $d_{Pd} = 3.0\,nm$ (a), $d_{Pd} = 2.0\,nm$ (b); $d_{Fe} = 2.0\,nm$, $d_{Pd} = 3.0\,nm$ (c), $d_{Pd} = 2.0\,nm$ (d).

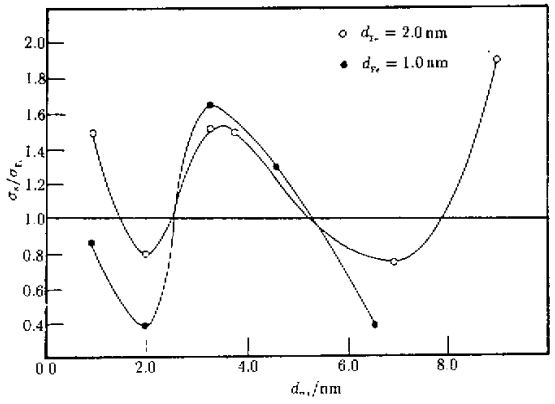


Fig. 6. Specific saturation magnetization as a function of Pd spacer thickness in $[Fe(1.0\,nm)/Pd(1.0–9.0\,nm)]_{40}$ and $[Fe(2.0\,nm)/Pd(1.0–9.0\,nm)]_{40}$. $\sigma_s^{Fe}$: specific saturation magnetization of 200 nm Fe layer.

For further investigating the relationship between magnetic polarization of Pd layers and the Pd layer thickness in Fe/Pd multilayers, we have measured the magnetic hysteresis loops of $[Fe(1.0\,nm)/Pd(1.0–9.0\,nm)]_{40}$ and $[Fe(2.0\,nm)/Pd(1.0–9.0\,nm)]_{40}$ multilayers. Figure 7 shows some magnetic hysteresis loops and Fig. 8 shows the dependence of specific saturation magnetization of $[Fe(1.0\,nm)/Pd(1.0–9.0\,nm)]_{40}$ and $[Fe(2.0\,nm)/Pd(1.0–9.0\,nm)]_{40}$ on Pd layer thickness. The results illustrate two characters: (a) The specific saturation magnetization of Fe/Pd multilayer structures oscillates with the increase of Pd layer thickness. (b) The oscillation in magnetization is around the specific saturation magnetization of Fe single layer. From (b) and the experimental formula (2), one can conclude that the interlayer coupling between Fe layers is ferromagnetic and no antiferromagnetic coupling appears with increasing Pd layer thickness. This is in accordance with the results of Parkin.[18] From Figs. 3 and 6, and character (a), it is suggested that there is obvious magnetic polarization of Pd layers and the polarization of Pd layers in Fe/Pd multilayer structures does change its sign, from positive to negative. That is to say, the magnetic exchange coupling between Fe and Pd layers oscillates between ferromagnetic and antiferromagnetic. It must be noted that this type of oscillatory coupling is different from that most reported in Fe(Co)/Cu(Cr, Ru) multilayer structures, which is the interlayer coupling oscillation between Fe(Co) layers. This coupling oscillation occurs between Fe and Pd layers, and the interlayer coupling between Fe layers keeps ferromagnetic. This is a new type of oscillation and the period of the oscillation is as large as about 4.0 nm.

## IV. THEORETICAL CALCULATION

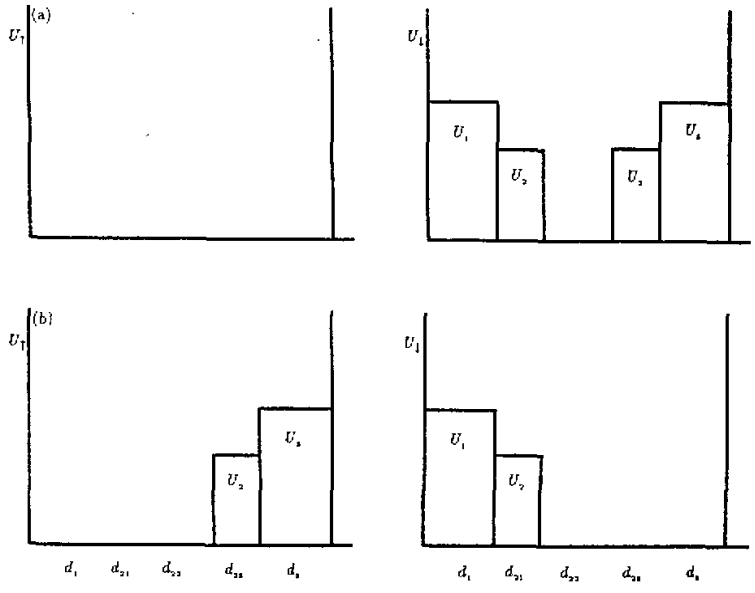


**Fig. 9.** Schematic illustration of the single electron effective potential for spin-up and spin-down electrons in the parallel (a) and antiparallel (b) configurations as the average polarization of spacer is positive.

For illustrating the possibility of this new type of coupling oscillation, we calculate the interlayer coupling behaviour of the Fe/Pd multilayer structures in the framework of Barnás model.[15] We will concentrate on the following questions: (a) how the magnetic polarization of a nearly ferromagnetic spacer influences the coupling between ferromagnetic layers and (b) how the coupling between the magnetic layer and spacer depends upon the thickness of the spacer. First, we calculate the interlayer coupling between Fe layers as the magnetic polarization of Pd spacer is positive. Second, we calculate the interlayer coupling between Fe layers as the magnetic polarization of Pd spacer is negative. Finally, the coupling between Fe and Pd layers is studied.

Now let us consider two ferromagnetic films with thicknesses $d_1$ and $d_3$, respectively, with a nearly ferromagnetic metal spacer of thickness $d_2$. The electrons are subject to spin-dependent effective potential wells as shown schematically in Figs. 9 and 10.

The exchange coupling $J$ between two ferromagnetic layers is calculated by comparing the total energy of parallel magnetic configuration of ferromagnetic layers with that of antiparallel alignment[15],

$$J = \Omega_{AF} - \Omega_{F} , \tag{4}$$

where $\Omega_{AF}$ and $\Omega_{F}$ are the thermodynamic potentials of the conducting electrons per unit

area for antiferromagnetic (AF) and ferromagnetic (F) alignments respectively. Taking into account the quasi-temperature limit, one obtains the following expression for $\Omega_\nu(\nu = \mathrm{F}, \mathrm{AF})$,

$$\Omega_\nu = \Omega_{\nu\uparrow} + \Omega_{\nu\downarrow} \tag{5}$$

and

$$\Omega_{\nu\sigma} = \frac{m}{2\pi\hbar^2} B_{\nu\sigma}(\mu\langle E_{\nu\sigma}\rangle - \frac{\mu^2}{2} - \frac{1}{2}\langle E^2_{\nu\sigma}\rangle) \,, \tag{6}$$

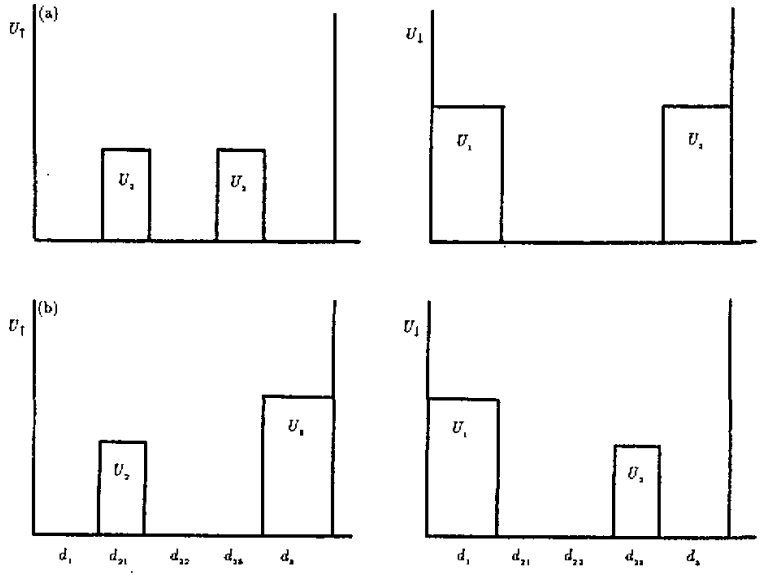


**Fig. 10.** Schematic illustration of the single electron effective potential for spin-up and spin-down electrons in the parallel (a) and antiparallel (b) configurations as the average polarization of spacer is negative.

for $\sigma = \uparrow, \downarrow, \mu$ is the chemical potential and is assumed to be constant at the transition from F to AF configurations due to high density of the d electron states at Fermi level. In Eq. (3), $\langle E_{\nu\sigma}\rangle$ and $\langle E^2_{\nu\sigma}\rangle$ are defined as

$$\langle E_{\nu\sigma}\rangle = \frac{1}{N_{\mu\sigma}} \sum_{n=1}^{N_{\nu\sigma}} \varepsilon^n_{\nu\sigma} \,, \tag{7}$$

$$\langle E^2_{\nu\sigma}\rangle = \frac{1}{N_{\mu\sigma}} \sum_{n=1}^{N_{\nu\sigma}} (\varepsilon^n_{\nu\sigma})^2 \,, \tag{8}$$

where $N_{\nu\sigma}$ is the total number of discrete energy levels below the Fermi energy for spin $\sigma$ and $\nu$th configuration, $\varepsilon^n_{\nu\sigma}$ the $n$th discrete energy level which results from the quantization of

perpendicular motion for spin $\sigma$ and $\nu$th configuration, which is determined by the following equation:

$$
\begin{aligned}
&kk_1k_2k_3\cos k_1d_1\cos k_2d_{21}\cos kd_{22}\cos k_3d_{23}\sin k_4d_3\\
&-kk_2k_2k_3\sin k_1d_1\sin k_2d_{21}\cos kd_{22}\cos k_3d_{23}\sin k_4d_3\\
&-kkk_1k_3\cos k_1d_1\sin k_2d_{21}\sin kd_{22}\cos k_3d_{23}\sin k_4d_3\\
&-kkk_2k_3\sin k_1d_1\cos k_2d_{21}\sin kd_{22}\cos k_3d_{23}\sin k_4d_3\\
&+kk_1k_2k_4\cos k_1d_1\cos k_2d_{21}\cos kd_{22}\sin k_3d_{23}\cos k_4d_3\\
&-kk_2k_2k_4\sin k_1d_1\sin k_2d_{21}\cos kd_{22}\sin k_3d_{23}\cos k_4d_3\\
&-kkk_1k_4\cos k_1d_1\sin k_2d_{21}\sin kd_{22}\sin k_3d_{23}\cos k_4d_3\\
&-kkk_2k_4\sin k_1d_1\cos k_2d_{21}\sin kd_{22}\sin k_3d_{23}\cos k_4d_3\\
&+k_1k_2k_3k_4\cos k_1d_1\cos k_2d_{21}\sin kd_{22}\cos k_3d_{23}\cos k_4d_3\\
&-k_2k_2k_3k_4\sin k_1d_1\sin k_2d_{21}\sin kd_{22}\cos k_3d_{23}\cos k_4d_3\\
&-kk_1k_3k_4\cos k_1d_1\sin k_2d_{21}\cos kd_{22}\cos k_3d_{23}\cos k_4d_3\\
&+kk_2k_3k_4\sin k_1d_1\cos k_2d_{21}\cos kd_{22}\cos k_3d_{23}\cos k_4d_3\\
&-k_1k_2k_3k_3\cos k_1d_1\cos k_2d_{21}\sin kd_{22}\sin k_3d_{23}\sin k_4d_3\\
&+k_2k_2k_3k_3\sin k_1d_1\sin k_2d_{21}\sin kd_{22}\sin k_3d_{23}\sin k_4d_3\\
&-kk_1k_3k_3\cos k_1d_1\sin k_2d_{21}\cos kd_{22}\sin k_3d_{23}\sin k_4d_3\\
&-kk_2k_3k_3\sin k_1d_1\cos k_2d_{21}\cos kd_{22}\sin k_3d_{23}\sin k_4d_3=0\,,
\end{aligned}
\tag{9}
$$

where

$$
k=\sqrt{2m\varepsilon/\hbar^2}\;;\quad k_i=\sqrt{2m(\varepsilon-V_i)/\hbar^2}\,,
\tag{10}
$$

$m$ is the mass of an electron.

### A. The case in which average polarization of spacer is positive

In this case, the spin-dependent effective potential wells, to which the electrons are subject, are shown schematically in Fig. 9.

In Fig. 9(a), the interlayer coupling between two ferromagnetic layers is ferromagnetic and in Fig. 9(b) it is antiferromagnetic. For simplicity, it has been assumed here that the bottom of spin majority conduction band in both ferromagnetic layers coincides with that in the nearly ferrimagnetic spacer.

In the case of Fig. 9(a),

$$
\begin{aligned}
&\text{spin}-\text{up}:\quad V_i=0\,,\quad i=1,2,3,4\,,\\
&\qquad\qquad K_i=k\,,
\end{aligned}
\tag{11}
$$

By inserting Eq. (11) into Eq. (9), one can obtain:

$$\cos k(d_1 + d_2)\sin kd_3 + \sin k(d_1 + d_2)\cos kd_3 = 0 \,. \tag{12}$$

$$\text{spin} - \text{down}: \quad V_1 = U_1 \,, \quad V_2 = V_3 = U_2 \,, V_4 = U_3 \,, \tag{13}$$

$$\begin{aligned}
&kk_1k_2^2 \sin k_1(d_1 + d_3)\cos k_2(d_{21} + d_{23})\cos kd_{22} \\
&+kk_1^2k_2 \cos k_1 d_1 \sin k_2(d_{21} + d_{23})\cos kd_{22}\cos k_1 d_3 \\
&-kk_2^3 \sin k_1 d_1 \sin k_2(d_{21} + d_{23})\cos kd_{22}\sin k_1 d_3 \\
&-k^2k_1^2 \cos k_1 d_1 \sin k_2 d_{21} \sin kd_{22} \sin k_2 d_{23} \cos k_1 d_3 \\
&-k_2^2k_1k_2 \cos k_1 d_1 \sin k_2 d_{21} \sin k_{22} \cos k_2 d_{23} \sin k_1 d_3 \\
&+k^2k_1k_2 \sin k_1 d_1 \cos k_2 d_{21} \sin kd_{22} \sin k_2 d_{23} \cos k_1 d_3 \\
&-k^2k_2^2 \sin k_1 d_1 \cos k_2 d_{21} \sin kd_{22} \cos k_2 d_{23} \sin k_1 d_3 \\
&+k_1k_2^3 \cos k_1 d_1 \cos k_2 d_{21} \sin kd_{22} \sin k_2 d_{23} \sin k_1 d_3 \\
&+k_1k_2^3 \sin k_1 d_1 \sin k_2 d_{21} \sin kd_{22} \cos k_2 d_{23} \cos k_1 d_3 \\
&+k^2k_2^2 \cos k_1 d_1 \cos k_2 d_{21} \sin kd_{22} \cos k_2 d_{23} \cos k_1 d_3 \\
&+k_2^4 \sin k_1 d_1 \sin k_2 d_{21} \sin kd_{22} \sin k_2 d_{23} \sin k_1 d_3 = 0 \,.
\end{aligned} \tag{14}$$

And for Fig. 9 (b),

$$\text{spin} - \text{up}: \quad V_1 = U_1 \,, \quad V_2 = U_2 \,, \quad V_3 = V_4 = 0 \,,$$

$$\begin{aligned}
&kk_3 \cos k(d_1 + d_{21} + d_{22})\cos k_3 d_{23} \sin k_4 d_3 \\
&+kk_4 \cos k(d_1 + d_{21} + d_{22})\sin k_3 d_{23} \cos k_4 d_3 \\
&+k_3k_4 \sin k(d_1 + d_{21} + d_{22})\cos k_3 d_{23} \cos k_4 d_3 \\
&-k_3^2 \sin k(d_1 + d_{21} + d_{22})\sin k_3 d_{23} \sin k_4 d_3 = 0 \,.
\end{aligned} \tag{15}$$

$$\text{spin} - \text{down}: \quad V_1 = V_2 = 0 \,, \quad V_3 = U_2 \,, \quad V_4 = U_3 \,,$$

$$\begin{aligned}
&kk_2 \sin k_1 d_1 \cos k_2 d_{21} \cos k(d_{22} + d_{23} + d_3) \\
&+kk_1 \cos k_1 d_1 \sin k_2 d_{21} \cos k(d_{22} + d_{23} + d_3) \\
&+k_1k_2 \cos k_1 d_1 \cos k_2 d_{21} \sin k(d_1 + d_{21} + d_{22}) \\
&-k_2^2 \sin k_1 d_1 \sin k_2 d_{21} \sin k(d_1 + d_{21} + d_{22}) = 0 \,.
\end{aligned} \tag{16}$$

The electronic energy spectra were obtained by solving Eqs. (12), (14), (15) and (16) numerically with a set of parameters $U_1 = U_3 = 5.0\,\text{eV}$, $U_2 = 3.0\,\text{eV}$, the chemical potential

$\mu = 2.7\text{eV}$, and $d_{21} = d_{23}$ is taken as 2ML according to measured data.[20] Then the coupling $J$ was obtained from Eqs. (4)–(8). Figure 11 shows the dependence of the calculated interlayer coupling $J$ on the thickness of spacer $d_2$ for the case in which polarization of the spacer is positive.

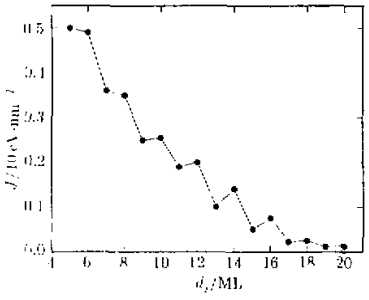


**Fig. 11.** Dependence of $J$ on spacer thickness $d_2$ as the average polarization of spacer is positive.

### B. The case in which average polarization of spacer is negative

As the interlayer coupling of magnetic layers keeps ferromagnetic [Fig. 9(a)],

$$\text{spin}-\text{up}: \quad V_1 = 0\,, \quad V_2 = V_3 = U_2\,, \quad V_4 = 0\,,$$

$$\begin{aligned}
&k^2k_2^2 \sin k(d_1 + d_{21} + d_3)\cos k_2 d_{21} \cos k_2 d_{23} \\
&-k^2k_2^2 \sin k(d_1 + d_3)\cos kd_{22} \sin k_2 d_{21} \sin k_2 d_{23} \\
&-kk_2^3 \sin kd_1 \sin k_2 d_{21} \cos k_2 d_{23} \sin k(d_{22} + d_3) \\
&+k^3k_2 \cos k(d_1 + d_{22})\cos k_2 d_{21} \sin k_2 d_{23} \cos kd_3 \\
&+k^3k_2 \cos kd_1 \sin k_2 d_{21} \cos k_2 d_{23} \cos k(d_{22} + d_3) = 0\,,
\end{aligned} \tag{17}$$

$$\text{spin}-\text{down}: \quad V_1 = U_1\,, \quad V_2 = V_3 = 0\,, \quad V_4 = U_3 = U_1\,,$$

$$\begin{aligned}
&k^2k_1^2 \cos k_1 d_1 \sin kd_2 \cos k_1 d_3 \\
&-k^4 \sin k_1 d_1 \sin kd_2 \sin k_1 d_3 \\
&+k^3k_1 \sin k_1(d_1 + d_3)\cos kd_2 = 0\,.
\end{aligned} \tag{18}$$

As the interlayer coupling between magnetic layers is antiferromagnetic [Fig. 10(b)], then

$$\text{spin}-\text{up}: \quad V_1 = 0\,, \quad V_2 = U_2\,, \quad V_3 = 0\,, \quad V_4 = U_3 = U_1\,,$$

$$
\begin{aligned}
&k^3 k_2 \cos k_2 d_{21} \sin k_4 d_3 \cos k(d_1 + d_{22} + d_{23}) \\
&-k^2 k_2^2 \sin k d_1 \sin k_2 d_{21} \sin k_4 d_3 \cos k(d_{22} + d_{23}) \\
&-k^3 \cos k d_1 \sin k_2 d_{21} \sin k_4 d_3 \sin k(d_{22} + d_{23}) \\
&+k^2 k_2 k_4 \cos k_2 d_{21} \cos k_4 d_3 \sin k(d_1 + d_{22} + d_{23}) \\
&-k k_2^2 k_4 \sin k_2 d_{21} \cos k_4 d_3 \sin k d_1 \sin k(d_{22} + d_{23}) \\
&+k^3 k_4 \sin k_2 d_{21} \cos k_4 d_3 \cos k d_1 \cos k(d_{22} + d_{23}) = 0 \, .
\end{aligned} \tag{19}
$$

$$
\text{spin} - \text{down}: \quad V_1 = U_1 \, , \quad V_2 = 0 \, , V_3 = U_2 \, , \quad V_4 = 0 \, ,
$$

$$
\begin{aligned}
&k^3 k_3 \sin k_1 d_1 \cos k_3 d_{23} \cos k(d_{21} + d_{22} + d_3) \\
&-k^4 \sin k_1 d_1 \sin k_3 d_{23} \cos k d_3 \sin k(d_{21} + d_{22}) \\
&-k^2 k_3^2 \sin k_1 d_1 \sin k_3 d_{23} \sin k d_3 \cos k(d_{21} + d_{22}) \\
&+k^2 k_1 k_3 \cos k_1 d_1 \cos k_3 d_{23} \sin k(d_{21} + d_{22} + d_3) \\
&-k k_1 k_3^2 \cos k_1 d_1 \sin k_2 d_{23} \sin k d_3 \sin k(d_{21} + d_{22}) \\
&+k^3 k_1 \cos k_1 d_1 \cos k_3 d_{23} \cos k d_3 \cos k(d_{21} + d_{22}) = 0 \, .
\end{aligned} \tag{20}
$$

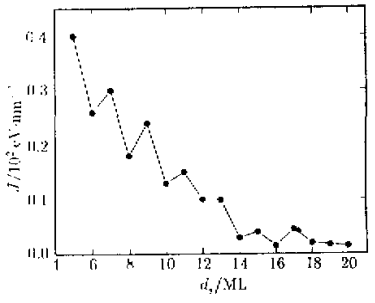


**Fig. 12.** Dependence of $J$ on spacer thickness $d_2$ as the average polarization of spacer is negative.

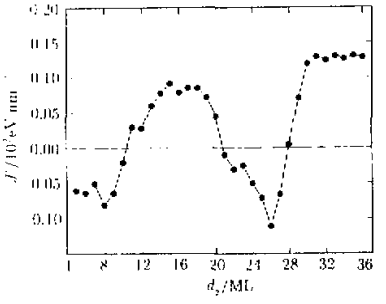


**Fig. 13.** Dependence of $J'$ on spacer thickness $d_2$.

Figure 12 shows the dependence of the calculated interlayer coupling $J$ on the thickness of spacer $d_2$ for the case in which polarization of the spacer is negative. From Figs. 11 and 12, it can be seen that in the calculated range of $d_2$, whether the polarization of spacer is positive or negative, the interlayer coupling between magnetic layers is always ferromagnetic, and no antiferromagnetic coupling between magnetic layers appears. This perhaps is the reason that no antiferromagnetic interlayer coupling was found in Fe/Pd and other Pd, Pt spaced layer structures investigated by Parkin *et al.* This means that the additional exchange coupling caused by the polarization effect of the nearly ferromagnetic spacer may restrain the antiferromagnetic interlayer coupling between magnetic layers. On the other hand, the

calculated $J$ decreases oscillatorily with $d_2$. The period of oscillation is about 0.4–0.5 nm. This is in accordance with the results of Fe/Pd/Fe sandwiches.[19]

### C. Comparison between the cases of positive and negative polarizations in spacer

From the above results, the states represented by Figs. 9(a) and 10(a), in which magnetic layers couples ferromagnetically, are the low energy states. Now we consider the energy difference between these two states by

$$J' = \Omega_F^{\mathrm{N}} - \Omega_F^{\mathrm{P}} , \tag{21}$$

where $F$ represents the ferromagnetic interlayer coupling between magnetic layers, P(N) represents the positive (negative) polarization in spacer.

The calculated $J'$ as a function of $d_2$ is shown in Fig. 13. $J'$ oscillates with increasing $d_2$, that is to say, both the states in Figs. 9(a) and 10(a) are stable ones and appear alternatively as the thickness of Pd layer is varied. Thus, this alternative polarization between positive and negative in the spacer would lead to the oscillation in magnetization of multilayers as the thickness of spacers is changed. This illustrates that the above analysis on the oscillation in magnetization of Fe/Pd multilayers is reasonable.

### D. Discussion

$U_2/U_1$ has great influences on the $J$-$d_2$ relation. If $U_2/U_1 \to 0$, as shown in Fig. 14(a), the spin-dependent effective potential well to which the electrons are subject is similar to that in the Barnas' calculation on Co/Cu multilayers [Fig. 14(b)], which gives oscillatory interlayer coupling between ferromagnetic layers. In this case, the polarization is too weak to restrain the antiferromagnetic interlayer coupling and the calculated $J$ oscillates with increasing $d_2$. If $U_2/U_1 \to 1$, as shown in Fig. 14(c), the spin-dependent effective potential well (within $d_{22}$) is also similar to that in Fig. 14(b), and the calculated $J$ would oscillate with $d_2$. If $U_2/U_1 \sim 0.5$ (0.6 for our calculations), then $J$-$d_2$ shows the relation like that in Figs. 11 and 12, the interlayer coupling between magnetic layers is always ferromagnetic. This suggests that the difference in polarization of spacers will lead to different exchange coupling in multilayer systems.

The chemical potential $\mu$ also shows influences on $J$-$d_2$. As the value of $\mu$ is in appropriate range, $J$ decreases with increasing $d_2$, but the sign of the interlayer coupling keeps positive. As $\mu$ increases, $J$ decreases with it and oscillates with $d_2$ between ferromagnetic and antiferromagnetic alternatively. The chemical potential $\mu$ is related to the interface structure. Therefore, in the same type of multilayer such as Fe/Pd, the difference of the interface structure made by different preparation techniques would cause the variation of

chemical potential $\mu$, and in turn lead to the variation of interlayer coupling.

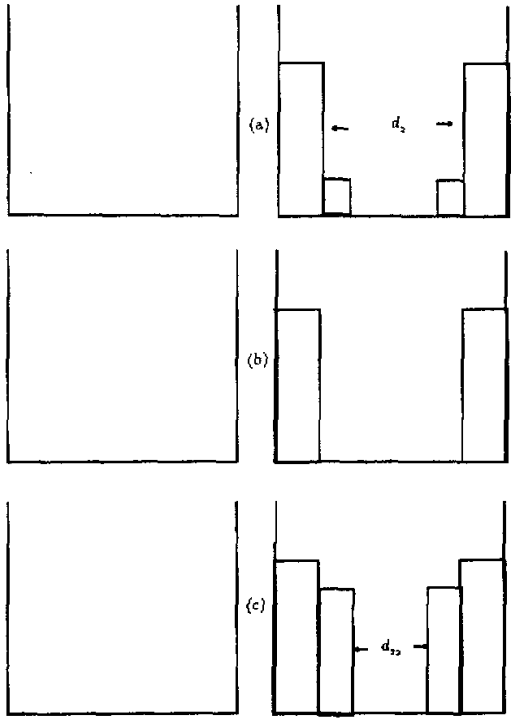


**Fig. 14.** Schematic illustration of the single electron effective potential for various $U_2/U_1$ cases. (a) $U_2/U_1 \to 0$. (b) $U_2 = 0$. (c) $U_2/U_1 \to 1$.

## V. CONCLUSIONS

The oscillation in magnetization of Fe/Pd multilayers prepared by evaporation as a function of the thickness of Pd layers is observed according to the measurements of VSM. By the analysis of data and CEMS measurements, we indicate that the oscillation in magnetization is caused by the polarization oscillation of Pd layers between positive and negative, and the Fe layers couples ferromagnetically. In the frame of Barnas model, the exchange coupling in ferromagnetic/nearly ferromagnetic multilayered structure is calculated. The results illustrate that the strong polarization of the spacer would restrain the interlayer antiferromagnetic coupling between ferromagnetic layers. Under an appropriate condition, the polarization of the nearly ferromagnetic layers would alternate positively and negatively with the increase of the thickness of nearly ferromagnetic layers, which causes the oscillation in magnetization of multilayers. Furthermore, it is indicated that the variation in strength of

polarization of the spacers and the difference of interface structures due to the preparation techniques would affect the character of the interlayer coupling in multilayers.

## REFERENCES


[1] P. Grunberg, R. Schreiber, Y. Pang, M. B. Bradsky and H. Sowers, *Phys. Rev. Lett.*, **57**(1986), 2442.

[2] A. Cebollada, J. L. Martinez, J. M. Gallego, J. J. de Miguel, A. Ferrer, F. Batallan and J. P. Rebouiliat, *Phys. Rev.*, **B39**(1989), 9726.

[3] B. Heinrich, Z. Celinski, J. F. Cochran, W. B. Muir, J. Rudd, Q. M. Zhong, A. S. Arrott, K. Myrtle and J. Kirschner, *Phys. Rev. Lett.*, **64**(1990), 673.

[4] S. S. P. Parkin, N. More and K. P. Roche, *Phys. Rev. Lett.*, **64**(1990), 2304.

[5] S. S. P. Parkin, R. Bhadra and K. P. Roche, *Phys. Rev. Lett.*, **66**(1991), 2152.

[6] C. Chappert and J. P. Renard, *Eur. Phys. Lett.*, **15**(1991), 553.

[7] P. Bruno and C. Chappert, *Phys. Rev. Lett.*, **67**(1991), 1602.

[8] M. W. Fairbairn and S. Y. Yip, *J. Phys.: Condens. Matter.*, **2**(1990), 4197.

[9] D. M. Edwards and J. Mathon, *J. Magn. Magn. Mat.*, **93**(1991), 85; D. M. Edwards, J. Mathon, R. B. Muniz and M. S. Phan, *Phys. Rev. Lett.*, **67**(1991), 493.

[10] P. M. Levy, K. Ounadjela, S. W. Zhang, Y. Wang, S. Semmers and A. Fert, *J. Appl. Phys.*, **67**(1990), 5914.

[11] D. Stoffler and F. Gautier, *Prog. Theor. Phys. Suppl.*, **101**(1990), 139.

[12] H. Hasegawa, *Phys. Rev.*, **B42**(1990), 2368; **B43**(1991), 10803.

[13] Y. Wang, P. M. Levy and J. L. Fry, *Phys. Rev. Lett.*, **65**(1990), 2732.

[14] C. Lacroix and J. P. Gavigan, *J. Magn. Magn. Mat.*, **93**(1991), 423.

[15] J. Barnas, *J. Magn. Magn. Mat.*, **111**(1992), L215.

[16] T. Moriya, *Prog. Theor. Phys.*, **34**(1965), 329.

[17] J. S. Konvel and J. B. Forsyth, *J. Appl. Phys.*, **40**(1969), 1359.

[18] S. S. P. Parkin, *Phys. Rev. Lett.*, **67**(1991), 3598.

[19] Z. Celinski and B. Heinrich, *J. Magn. Magn. Mat.*, **99**(1991), L25.